Secondary Electrons from X-Ray Photocathodes

Sid Ghosh

Secondary Electrons from X-Ray Photocathodes

S. Ghosh
Advisor: Dr. P.A. Jaanimagi

University of Rochester
LABORATORY FOR LASER ENERGETICS
250 East River Road
Rochester, NY 14623-1299

ABSTRACT

Streak cameras are used to study the x-rays that are emitted from Inertial Confinement Fusion (ICF) targets as they implode. These cameras operate by using a photocathode to convert the x-ray flux to a secondary electron current. Secondary electrons are then focused onto a phosphor screen using the streak tube electron optics, and finally recorded using a charged coupled device (CCD) camera. The pulse height distributions for the number of secondary electrons per each absorbed x-ray event in the photocathode can be traced from the CCD data. Several photocathode materials were tested for their secondary electron number distributions by using a DC x-ray source and a slow ramp to uniformly illuminate the streak camera. The data was analyzed by generating histograms of the values of CCD superpixels that integrated the recorded signal in the pixels surrounding an x-ray event. The distribution for the number of secondary electrons produced per each absorbed x-ray event can then be derived by using the distribution for the number of CCD electrons recorded per single streak tube electron.

1. INTRODUCTION

X-ray streak cameras are used at the Laboratory for Laser Energetics (LLE) to serve as a diagnostic tool in inertial confinement fusion (ICF) experiments. The uniformity of a target's implosion can be studied by analyzing the x-ray emission that it produces. This is an important factor in determining the success of direct drive experiments in which the target needs to be

uniformly compressed.[1] The characterization of the x-ray diagnostics is important to the ICF program because it allows for better measurement and detection capabilities. By understanding the properties that govern the operation of the streak camera components, the system performance can be improved upon for greater accuracy. [2]

The PJx streak camera, built at LLE, was used for this work. The basic components of the streak camera system include the photocathode, streak tube and the CCD camera that is used to read the image into the computer. The streak tube operates on the principle of the photoelectric effect. X-ray photons create high-energy primary electrons, which in turn produce low energy secondary electrons. The secondary electrons are emitted from the photocathode surface and then focused through the streak tube. The streak tube consists of an electron optic system that relays an image of the photocathode to a phosphor screen. The PJx uses a quadrupole doublet lens for optimal focusing capabilities. The tube also includes a deflection system to sweep the electron beam across the screen (see Fig. 1). The light from the phosphor is fiber coupled to the CCD camera for maximum transfer efficiency. The PJx streak camera incorporates a Spectral Instruments 800 Series CCD Array Scientific Imaging Camera. [3] The x-ray source used in this experimentation was built by a previous summer student. It is a large area source; the x-ray flux is produced by 4 keV electrons bombarding a gold anode.[4]

The major component of the CCD camera is the CCD chip which contains a 2-dimensional pixel array to receive the incident light. This light is allowed to accumulate as charge in the wells of the pixels. The charge produced is proportional to the integral of the light intensity during the exposure time. Collected charge is then transferred to an output amplifier. This creates a measurable voltage signal proportional to the charge. The voltage is sent through an analog to digital converter, which converts the signal to Analog to Digital Units (ADUs). This

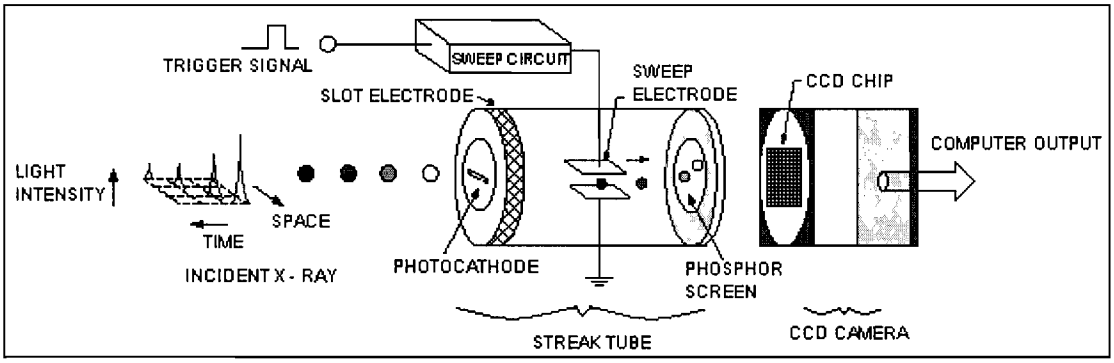

Fig. 1. Incident light is collected on the photocathode with respect to space and then swept across the phosphor screen of the streak tube in time.

output is then sent to the computer, where the image is displayed in terms of ADUs.

Various photocathode materials create different number distributions of streak tube secondary electrons. A method requiring several steps has been used to find the number of secondary electrons produced per single x-ray event. Streak data must first be generated using the DC x-ray source and a slow (0.5 s) streak ramp. The flux levels are kept sufficiently low so that individual absorbed x-rays are recorded as isolated events; less than 5% of the CCD pixels are illuminated in any one frame. The data is background subtracted and compiled into superpixel histograms. The superpixels integrate the energy in the pixels surrounding a given event. The histograms from multiple streak images are then summed together in order to improve the signal to noise ratio (SNR). Each histogram is the sum of the distributions of ADU values produced for 0 - n electron events. In order to derive the secondary electron number distributions, the ADU distributions for zero and single electron events needed to be found first.

2. CCD CALIBRATION

The CCD camera must first be calibrated in order to take accurate measurements of the secondary electron output. The background noise level, system gain (CCD electrons/ ADU) as well as the linearity of the A/D need to be measured. These values will determine the authenticity of the collected data.

Noise in the CCD can be attributed to several factors. The biggest contribution to the background is the read noise from the A/D digitization process. The read noise should be Gaussian distributed. A second source of background noise is from dark current, which is thermally generated charge that accumulates in the CCD wells during exposure times. Noise created by dark current is Poisson distributed. To avoid the accumulation of dark charge, the CCD camera is thermoelectrically cooled to a temperature of –40 °C, where the dark charge is almost negligible. Another source of noise is from cosmic ray hits. These hits produce very large pixel values that can be easily eliminated during the data analysis.

In Fig. 2, we present the resulting histogram from the subtraction of a pair of background frames. This data is well fit by a Gaussian distribution centered about a value of 0 ADUs, with a standard deviation (σ) of 7.95 ADUs (or 8.67 CCD electrons). This σ value is relatively small, so it indicates that our CCD camera is a good detector with low noise. The data collected here is for a readout speed of 200 kHz in the camera.

Poisson statistics describes the distribution for the number of photons incident upon a unit of area per a unit of time. When photons are absorbed in the CCD array, the resulting CCD electrons are also Poisson distributed. Using the principle that under Poisson statistics the variance is equal to the mean of the data, we can find the gain of the system and verify its linearity. A green LED light source was used to uniformly illuminate the CCD array for the data collection. The variance was calculated from the subtraction of a pair of data frames, while the mean signal was found by subtracting a background frame from a data frame. The exposure levels were varied by adjusting the duration of the LED pulse. Figure 3 shows the plot of the variance vs. mean and the straight line fit to the data.

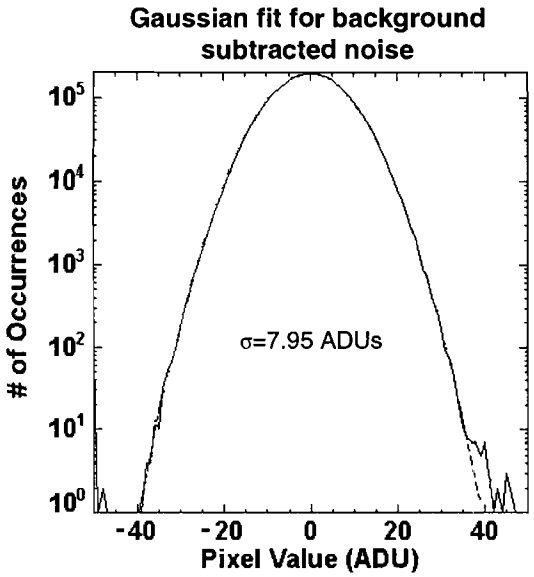

Fig. 2. Background subtracted frames produce a Gaussian distribution.

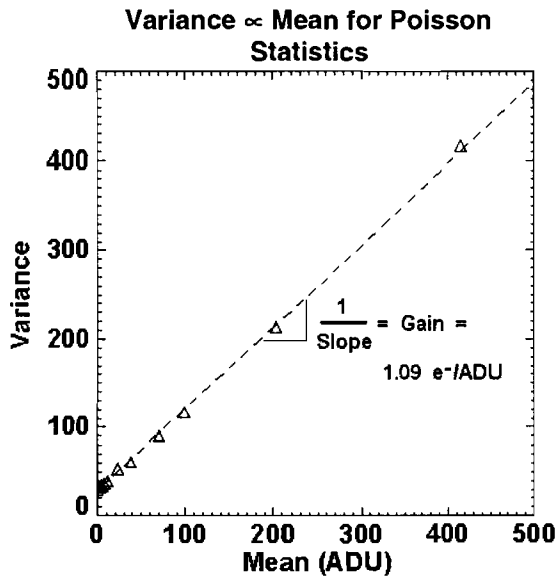

Fig. 3. Variance vs. Mean data produces a linear relationship.

To find the linear relationship for the data, a least squared fit was used, where:

$$(x_i, y_i) \qquad y = a_o + a_1 x$$

$$\chi^2 = \sum (a_o + a_1 x_i - y_i)^2 = \min. \tag{1}$$

The inverse of the slope for the line in this plot is equal to the CCD gain, which was found to be 1.09 CCD electrons per ADU.

3. STREAK IMAGES

Typical streak images are presented in Fig. 4, where each spot represents an absorbed x-ray event. The range of spot intensities and sizes corresponds to the distribution of the number of CCD electrons generated per single streak tube electron convolved with the number distribution of secondary electrons produced per absorbed x-ray. The spots are sparsely scattered throughout the image, so single events can be analyzed.

As is illustrated in Fig. 5, the 1x1, or normal pixel size does not capture the entire recorded signal from an event. The phosphorescence from a single electron event, even if it is centered on a single pixel, will generally be distributed among many pixels. Multiple secondary

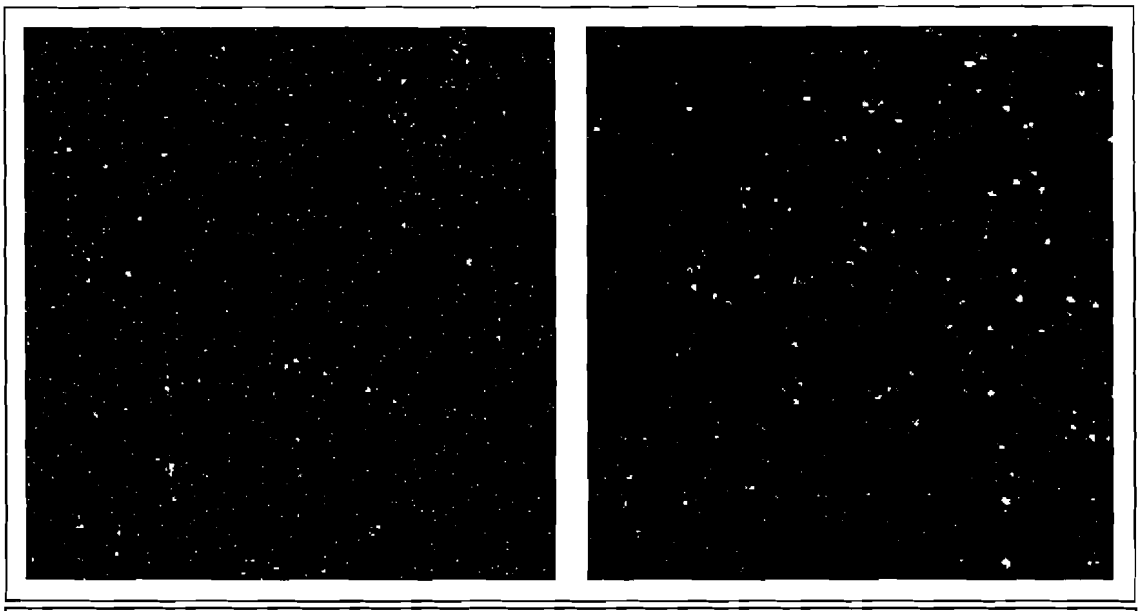

Fig. 4. The image on the left shows the secondary electron distribution from the Gold photocathode, while the image on the right shows the Potassium Bromide photocathode. The spots indicate secondary electron events. Both images are background subtracted and taken from streak tube operations of –25 kV. They are both 400 x 400 pixels of the CCD array in size.

electron events will spread their signal even further since the individual electrons will be imaged to different points on the phosphor screen, (dependent on their initial position and velocity vector at the photocathode). To ensure that the entire signal from a given event is integrated, superpixels centered about a local maximum pixel are created. The different superpixel sizes that were implemented in this study included 3x3, 5x5, 7x7 and 9x9 superpixels.

4. PHOTOCATHODE MATERIALS

Several photocathode materials were experimented with to find their secondary electron number distribution per absorbed x-ray event. Metals in addition to insulators were tested. The metals included aluminum, gold and beryllium. Aluminum was used because it forms an aluminum oxide layer rather quickly, and therefore a stable material for use as a photocathode. Gold was used because of its stability and x-ray absorption characteristics. Beryllium was tested simply because it was a material that was available at the time of experimentation. The insulators included potassium bromide (KBr) and "fluffy" KBr. KBr is a commonly used photocathode material with higher quantum efficiency and a narrower secondary electron energy distribution

than metal photocathodes. The fluffy type of the photocathode is produced by coating the material in an Argon atmosphere. The resultant coating has a lower density and higher quantum efficiency than standard KBr. Data was collected at streak tube potentials of –15 kV as well as –25 kV. This will affect the gain for recording single electron events but should not affect the secondary electron number distribution. The following photocathodes and conditions were used for experimentation:

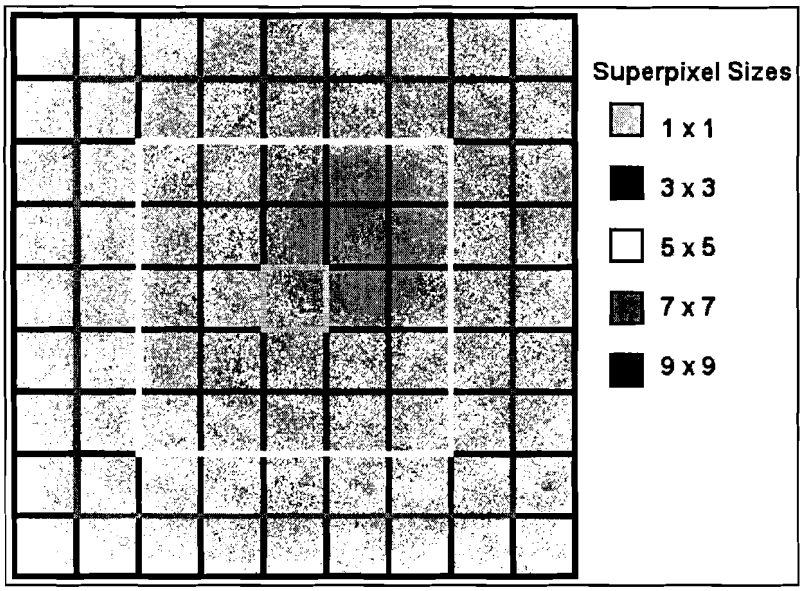

Fig. 5. Superpixels are created about a peak value (not the center of the distribution), and integrate the ADU values for the pixels surrounding the center.

Material:	Thickness:	Streak tube Potential:
Potassium Bromide (KBr)	1500 angstroms (Å)	-15 kV
Aluminum (Al)	2000 Å	-15 kV
Fluffy KBr	-	-15 kV
Gold (Au)	300 Å	-15 kV
Fluffy KBr	-	-25 kV
Au	300 Å	-25 kV
KBr	1500 Å	-15 kV, inverse
KBr	1500 Å	-25 kV, inverse
Beryllium (Be)	12.7 microns (μ)	-15 kV, inverse
Be	12.7 μ	-25 kV, inverse

The inverse mode operation of the streak camera produces a tighter focus of the electron beam in the time direction. The distribution for recording single electron events was generated using an aluminum photocathode illuminated with a mercury light source. The mercury source produces

ultraviolet radiation that is much lower in energy than x-rays, thus allowing for the release of single photoelectrons from the photocathode.

5. SUPERPIXEL HISTOGRAMS

The superpixel histograms were generated by first ordering the pixel values in the background subtracted image from maximum to minimum. Starting with the maximum pixel value and proceeding down to a threshold value of 5 ADU, the superpixel value is calculated as the sum of the 3x3 to 9x9 neighboring pixels. The original pixel values are then replaced with a random value selected from a Gaussian distribution with σ = 7.95 ADU, (see Fig.2). This allows us to avoid multiple counting of events. Since the data is sparse, the superpixel histograms are dominated by the N=0 electron component, i.e. background which we may define as D0. The N=1 electron component is added as the D1 distribution convolved with the background, D0. The N=2 electron component is added as the D2 (= D1 convolved with D1) distribution convolved with the background, D0, and so on for the N>2 electron components. As the superpixel size increases, a greater amount of energy is integrated and therefore the range of the data values in

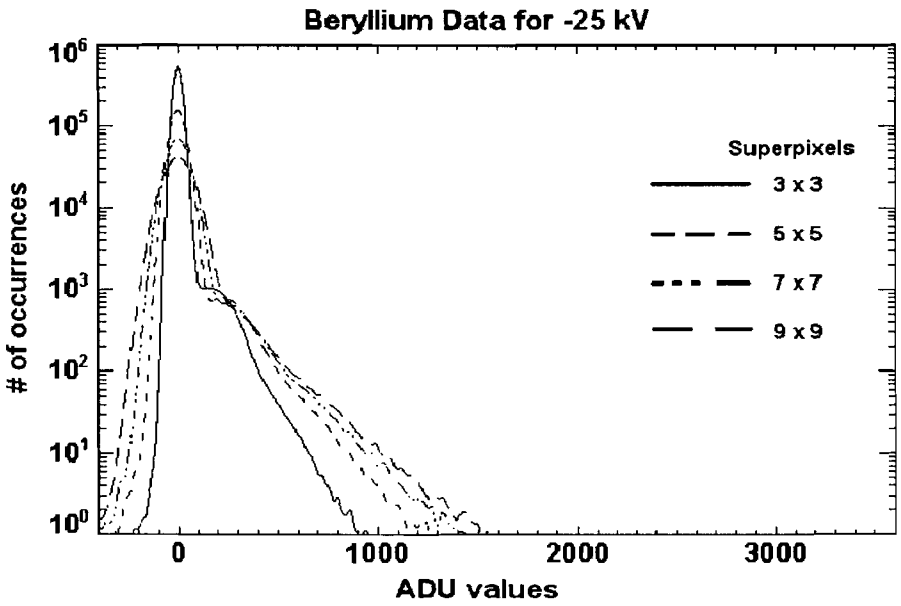

Fig. 6. Be data demonstrates visible signal on wing.

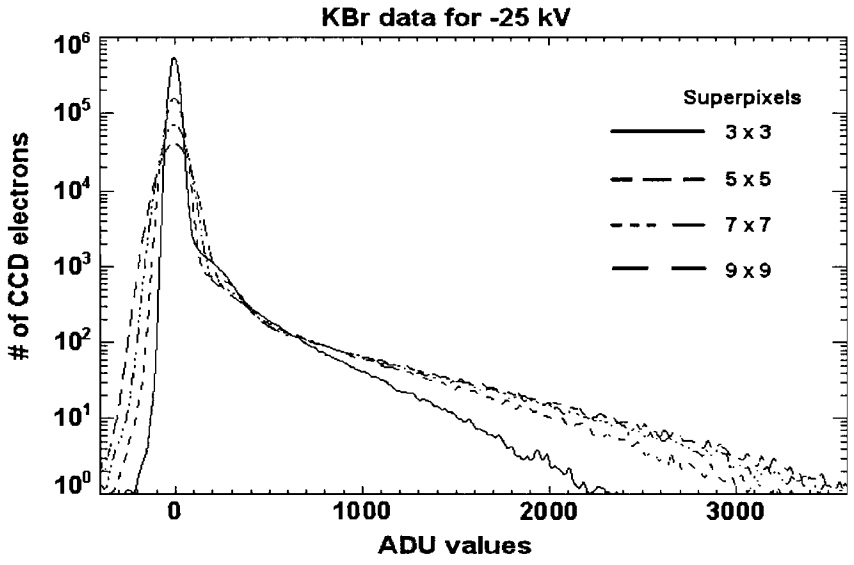

Fig. 7. KBr data extends out much farther, because the KBr photocathode produces a greater number of secondary electron events

ADUs increases as well. Also, the σ for the background Gaussian (D0) varies with the square root of the number of pixels in the superpixel. The histograms of the Be dataset are given in Fig. 6. The KBr data (Fig. 7) has a wing that extends out much farther than in the Be histogram. This is indicative of the fact that the signal is present through the N=15 secondary electron component. The shelf (near 200 ADU) that can be seen for the 3x3 superpixel in the Be and KBr histograms shows that the single electron event distribution is centered somewhere in that region, but is not clearly visible because of the large background signal.

6. QUANTUM EFFICIENCY AND TRANSMISSION

Another consideration in finding the number of secondary electrons produced can be made by calculating the quantum efficiency and transmission of the photocathode. Quantum efficiency is the probability that an electron will be released from a photocathode and is equal to the ratio of the number of electrons produced to the number of incident photons. It is proportional to the energy absorbed in the photocathode. Transmission represents the photons that go through the

photocathode without being absorbed. The transmission for a photocathode can be calculated through the formula:

$$Transmission = \frac{I_T}{I_O} = e^{(-\mu \rho x)} \tag{2}$$

where μ is equal to the mass absorption coefficient, ρ is the density and x is the effective secondary escape depth of the photocathode.[5] Absorption can be represented by 1-Transmission. Therefore the ratio of quantum efficiency to the absorption is equal to the number of secondary electrons produced.

$$\#Secondary\ Electrons = \frac{Quantum\ Efficiency}{1 - Transmission} \tag{3}$$

The plots for the transmission and quantum efficiency for 1500 Å KBr were found. (see Fig. 8)

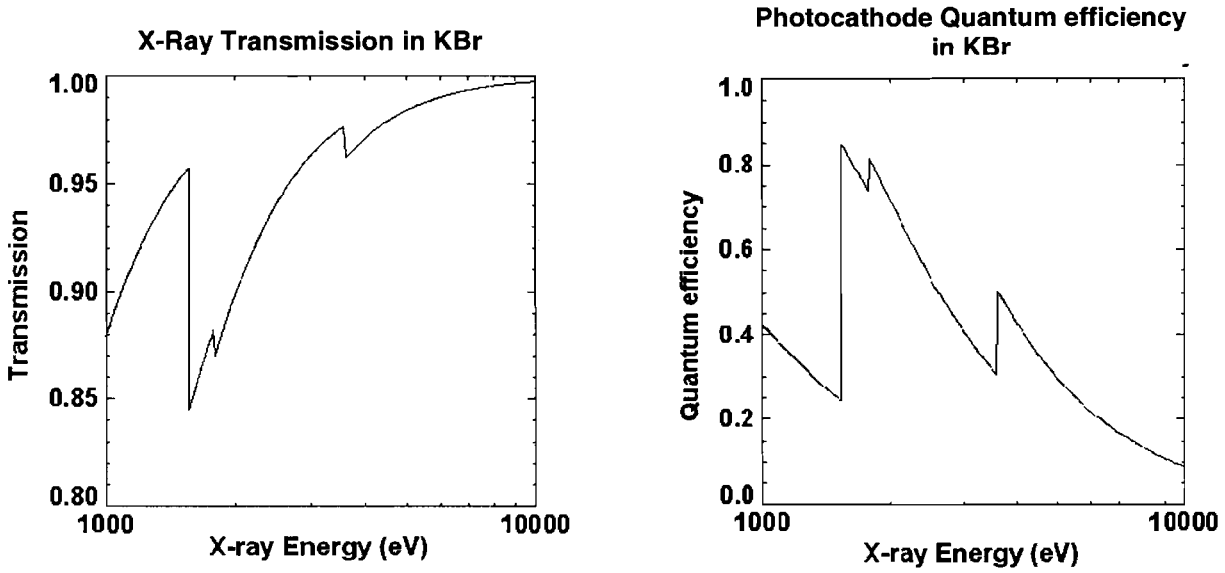

Fig. 8. X-Ray transmission and quantum efficiency plots for KBr (1500 Å).

The upper bound for our x-ray energy is set by the 4 keV electrons bombarding the gold anode in our x-ray source. The lower bound is 1 keV obtained from the transmission plot for Beryllium. In the range of 1-4 keV, the expected secondary electron production for KBr is approximately 3.5 to 14. These numbers however, do not correspond to the results we received for secondary electron

production. This may be due to the aging of the KBr photocathode; its response will degrade when exposed to atmospheric conditions. Since the calculations are made for an ideal situation, the discrepancy between the calculated results and the experimental results may be attributed to the degradation of the photocathode.

7. DATA ANALYSIS

In the superpixel histograms the data is in the form of:

$$Signal \otimes Background = Data. \tag{4}$$

where ⊗ denotes convolution. To find the signal, the background must be deconvolved from the data. This can be done through a Fast Fourier Transform (FFT). If the FFT is taken for the signal, background and the data, then the signal times the background should equal the data. The deconvolution can then be made through a division in Fourier space. When this procedure was applied to the data however, erroneous results were produced. The signal is lost in the noise

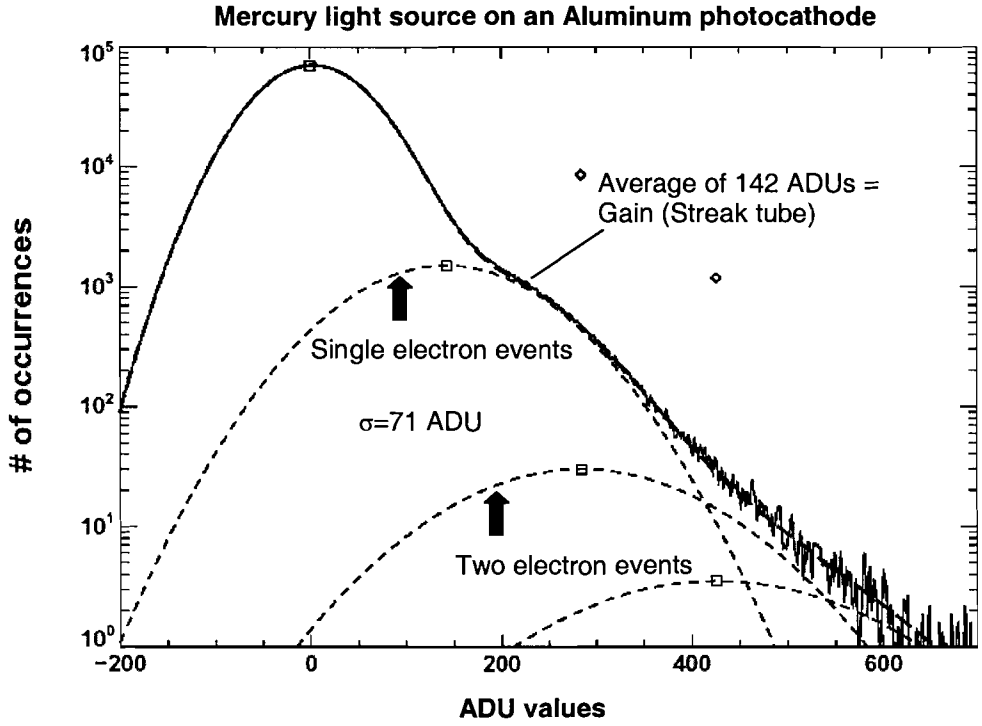

Fig. 9. The single electron event distribution is shown for the UV data. An average value of 142 ADUs is found signifying streak tube gain.

because the zero electron component is so much larger than any of the secondary electron components. Therefore the alternative process used was to find the single photoelectron distribution from the UV data and then apply the average found to predict the centers for multiple secondary electron events. The distribution for single electron events was found (see Fig. 9) from the Aluminum data taken with the mercury light source. The single photoelectron distribution is well fit by a Gaussian centered about an average of 142 ADUs, and a σ of 71 ADU. This signifies the gain for the streak tube, and states that on average, 142 ADUs are produced per streak tube electron (or 1 photoelectron). The ADU values can then be converted to CCD electrons by the gain of the CCD camera. Now we can predict 284 ADUs will be produced for 2 electron events, 426 ADUs for 3 electron events and so on. The ADUs per single electron event has now given the centers for the distributions in the other superpixel histograms. In order to find the signal, the amplitudes for the distributions at each electron event location can be subtracted from the data to

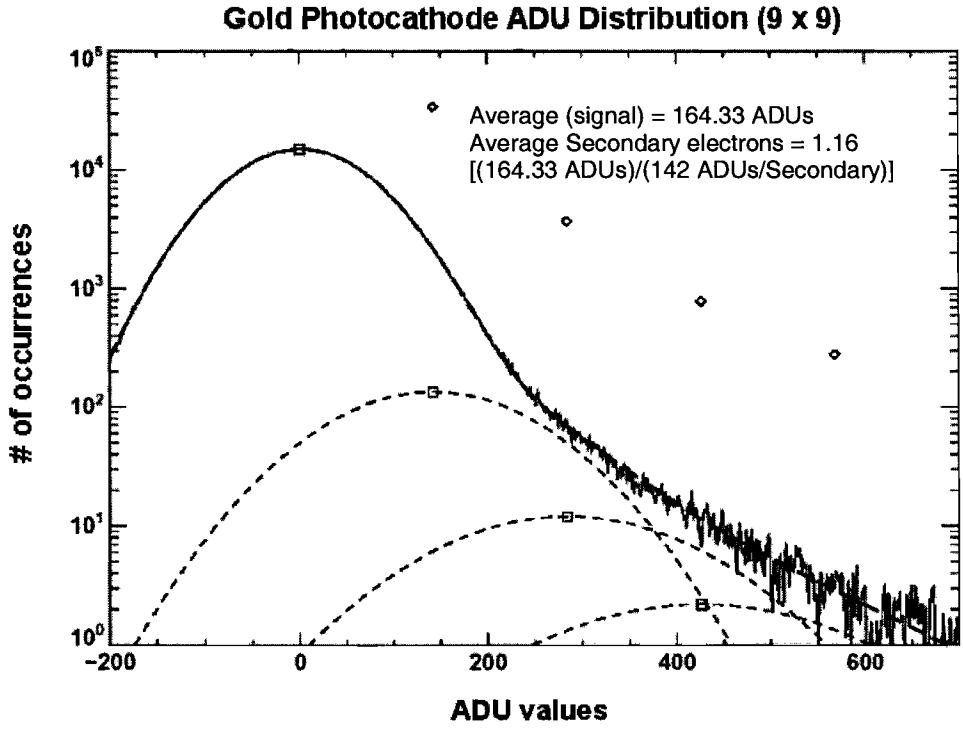

Fig. 10. The average of the gold data signal is found to be 162.62 ADUs. Applying the streak tube gain, the average secondary electrons produced is 1.16. The probability of 1 : 2 : 3 : 4 electron events is 0.877 : 0.095 : 0.020 : 0.007. The relative probability is shown as ◊ in the figure.

drive the residual (difference between the signal and the data) to 0. The secondary electron event distributions were found through four events for the 9x9 superpixel size of the gold photocathode. (see Fig. 10) When the background is removed from the gold data and only the signal composed of the multiple secondary electron events is left, an average signal of 164.33 ADUs with a signal to nose ratio (SNR) of 1.33 is obtained. Dividing out the streak tube gain allows us to find that the average secondary electron production per x-ray event in the gold photocathode is 1.16. The same process is applied to the 9x9 superpixel information in KBr. The primary difference is that KBr produces up through 15 secondary electron events, as was predicted from the elongated wing. (see Fig. 11)

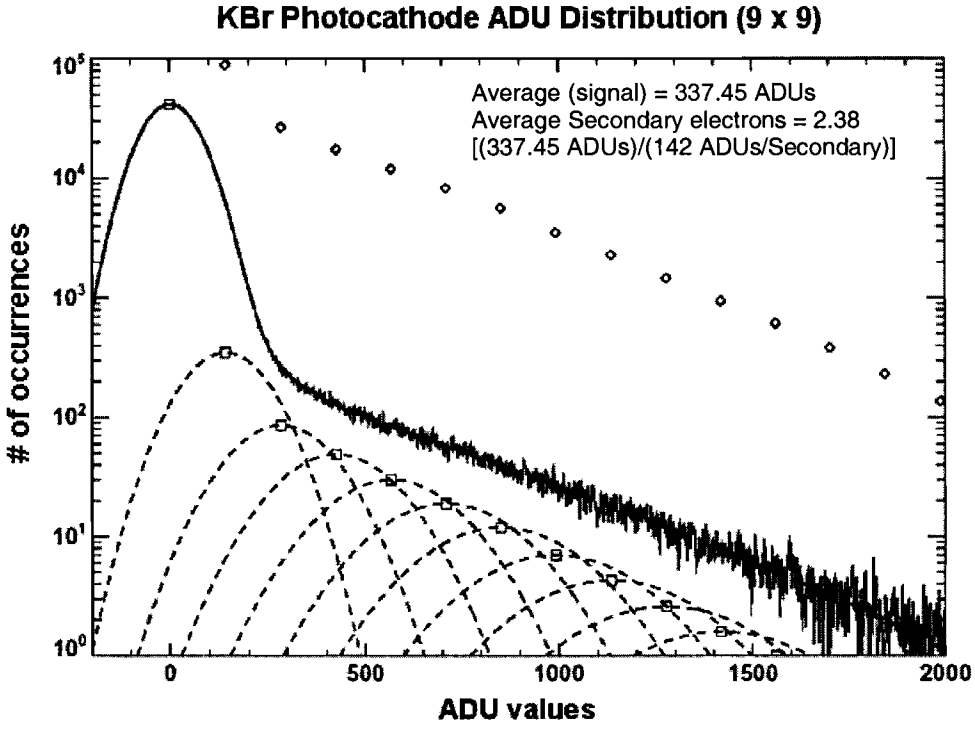

Fig. 11. The average secondary electron production in KBr is found to be 2.38. The signal extends through 15 electron events. The probability of 1 : 2 : 3 : ... events is 0.527 : 0.158 : 0.104 : ..., decreasing approximately by 0.68 for additional electrons.

For the KBr data, the average signal is found to be 337.45 ADUs with an SNR of 1.04, making the average secondary electron production per x-ray event 2.38.

8. DISCUSSION

After finding the single photoelectron distribution in ADUs per streak tube electron, the signal for the superpixel data was deconvolved. The photoelectron information allows us to correlate quantitatively the CCD data to the electron current in the streak tube. For single electron events, the σ is 71 ADU, which happens to equal half the streak tube gain for an SNR of 2.0. The generation of multiple secondary electrons per x-ray event degrades the SNR. Furthermore the secondary electron number distribution per x-ray event was measured for the Gold and KBr photocathodes, but the photoelectron information can be extended to find the distributions for the other photocathodes as well. The main significance of this finding, however, is that now measurements of the secondary electron distribution in CCD electrons will allow for the absolute calibration of the x-ray streak camera. With the Gold and KBr photocathodes as examples, we can now trace the CCD electron distribution all the way back to the absorbed x-rays because the secondary electron distribution per x-ray event has been found.

For future experimentation, we can work on finding the quantum efficiency for the photocathode from the secondary electron distribution. This can be done through the use of a monochromatic x-ray source, which will deliver only one energy and not a range as was used in this experimentation (1-4 keV). This will allow us to monitor the photocathode and the streak camera system and maintain the best diagnostics.

9. ACKNOWLEDGEMENTS

I would like to thank Dr. R. Stephen Craxton for giving me the opportunity to participate in this program. It has truly been an incredible experience for me. Next I would like to thank Mr. Robert Boni for the help he provided me during the first week of the program and later on as well. I would also like to thank Mr. Steven Noyes for taking the time to coat the photocathode materials that were used in the experimentation. Most of all I would like to thank my advisor, Dr. Paul

Jaanimagi for all the time and help he provided me in this project. Without his patience and many clarifications, this work would not have been possible for me.

10. REFERENCES

1. R.L. McCrory et al., "Omega ICF Experiments and Preparation for Direct-Drive Ignition on NIF", Nucl.Fusion, 41, 1413 (2001).
2. W.R. Donaldson, R. Boni, R.L. Keck and P.A. Jaanimagi, "A self-calibrating multichannel streak camera for inertial confinement fusion applications," in the *Review of Scientific Instruments*, Vol. 73, pg. 2606, July 2002.
3. "800 Series Camera System User's Manual," Spectral Instruments Inc., Tucson, Arizona, 2000.
4. A. Campanella, "Large Area, Low Voltage X-Ray Source," LLE Summer Program, 2000.
5. B.L. Henke, J.P. Knauer and K. Premaratne, J. Appl. Phys. 52, 1509, 1981.